



1 Carbon isotopic signature of coal-derived methane 2 emissions to atmosphere: from coalification to alteration 3

4 Giulia Zazzeri¹, Dave Lowry¹, Rebecca E. Fisher¹, James L. France^{1,2}, Mathias Lanoisellé¹, Bryce F.J. Kelly⁴,
5 Jaroslaw M. Necki³, Charlotte P. Iverach⁴, Elisa Ginty⁴, Mirosław Zimnoch³, Alina Jasek³ and Euan G. Nisbet¹.

6 ¹Royal Holloway University of London, Egham Hill, Egham, Surrey TW20 0EX

7 ²University of East Anglia, Norwich Research Park, Norwich, Norfolk NR4 7TJ

8 ³AGH-University of Science and Technology, Al.Mickiewicza 30 Kraków, Poland

9 ⁴Connected Waters Initiative Research Centre, UNSW Australia

10
11 *Correspondence to:* Dr Giulia Zazzeri (Giulia.Zazzeri.2011@live.rhul.ac.uk)

12 Prof Euan Nisbet (e.nisbet@es.rhul.ac.uk)

13
14 **Abstract.** Currently, the atmospheric methane burden is rising rapidly, but the extent to which shifts in coal
15 production contribute to this rise is not known. Coalbed methane emissions into the atmosphere are poorly
16 characterised, and this study provides representative $\delta^{13}\text{CCH}_4$ signatures to be used in regional and global models
17 in order to allow better apportionment of fossil fuel emissions. Integrated methane emissions from both
18 underground and opencast coal mines in the UK, Australia and Poland were sampled and isotopically
19 characterised. Progression in coal rank and secondary biogenic production of methane due to incursion of water
20 are suggested as the processes affecting the isotopic composition of coal-derived methane. An averaged value of
21 -65‰ has been assigned to bituminous coal exploited in open cast mines and of -55‰ in deep mines, whereas
22 values of -40‰ and -30‰ can be allocated to anthracite opencast and deep mines respectively. However, the
23 isotopic signatures that are included in global atmospheric modelling of coal emissions should be region or
24 nation specific, as greater detail is needed, given the wide global variation in coal type.

25 1 Introduction

26 Methane emissions from the energy sector have been driven in recent years by the impact of a shift from coal to
27 natural gas, in the US, in the UK and Eastern Europe, whereas in China coal production has increased in this
28 century. Currently, the atmospheric methane burden is rising rapidly (Nisbet et al., 2014), but the extent to
29 which shifts in coal production contribute to this rise is not known. Coalbed methane emissions into the
30 atmosphere are poorly characterised, as they are dispersed over large areas and continue even after the mines'
31 closure (IPCC, 2006). Methane is emitted in coal processing (crushing and pulverisation) and during the initial
32 removal of the overburden; it can be diluted and emitted through ventilation shafts in underground coal mines,
33 or directly emitted to atmosphere from open-cut coal mining, where releases may occur as a result of
34 deterioration of the coal seam.

35 For the UN Framework Convention on Climate Change, national emissions are estimated by a “bottom-up”
36 approach, based upon a general equation where the coal production data are multiplied by an emission factor
37 that takes into account the mine’s gassiness, which in turn is related to the depth of the mine and the coal rank
38 (i.e. carbon content of coal) (U.S. EPA, 2013). These modelled estimates are often calculated without an error



39 assessment, and therefore the level of accuracy of the emissions is not known. “Top-down” assessment of
40 methane emissions can be made by chemical transport models constrained by atmospheric measurements
41 (Bousquet et al., 2006; Locatelli et al., 2013). However, this top-down approach provides the total amount of
42 methane emissions into the atmosphere, which has to be distributed among the different methane sources in
43 order to quantify each source contribution.

44 For methane emissions from fossil fuels (coal and natural gas), the source partitioning is mainly “bottom-up”,
45 based on energy use statistics and local inventories, which might be highly uncertain. Conversely, the “top-
46 down” study of the carbon isotopic composition of methane, which is indicative of the methane origin, provides
47 a valuable constraint on the budget appraisal, allowing different sources in a source mix to be distinguished and
48 their individual strength to be evaluated (Liptay et al., 1998; Lowry et al., 2001; Townsend-Small et al., 2012).

49 Measurements of methane mole fractions can be complemented in atmospheric models by typical $\delta^{13}\text{CCH}_4$
50 signatures of the main methane sources in order to estimate global and regional methane emissions and assess
51 emissions scenarios throughout the past years (Fung et al., 1991; Miller, 2004; Whiticar and Schaefer, 2007;
52 Bousquet et al., 2006; Monteil et al., 2011; Mikaloff Fletcher et al., 2014). However, even though isotopic
53 values are fairly distinctive for specific methanogenic processes, the variety of production pathways and local
54 environmental conditions that discriminate the methane formation process leads to a wide range of $\delta^{13}\text{CCH}_4$
55 values. The global isotopic range for coal is very large, from -80 to -17 ‰ (Rice, 1993), but it can be narrowed
56 down when a specific basin is studied. While there are several studies of isotopic composition of methane
57 generated from coal in Australia, U.S.A. and China (Smith and Rigby, 1981; Dai et al., 1987; Rice et al., 1989;
58 Aravena et al., 2003; Flores et al., 2008; Papendik et al., 2011), there is a significant lack of information about
59 the isotopic characterisation of methane emissions from coal mines in Europe.

60 The purpose of this study was to determine links between $\delta^{13}\text{CCH}_4$ signatures and coal rank and mining setting,
61 and to provide representative ^{13}C signatures to be used in regional and global atmospheric models in order to
62 produce more accurate methane emission estimates for the coal exploitation sector.

63 1.1 Process of coalification and parameters affecting the $\delta^{13}\text{C}$ signature of methane emissions

64 The process of coalification involves both biochemical and geochemical reactions. The vegetal matter firstly
65 decays anaerobically under water; the simple molecules derived from initial decomposition (i.e. acetate, CO_2 ,
66 H_2 , NH_4^+ , HS^- , long chain fatty acids) are metabolised by fermentative archaea, which produce methane via two
67 methanogenic paths, acetoclastic reaction or CO_2 reduction (Whiticar, 1999). Different pathways lead to diverse
68 $\delta^{13}\text{CCH}_4$ isotopic signatures - methane from acetate is ^{13}C enriched relative to methane from CO_2 reduction,
69 ranging from -65 ‰ to -50 ‰ and -110 ‰ to -50 ‰ respectively (Levin et al., 1993; Waldron et al., 1998). With
70 increasing burial and temperatures, coal is subjected to thermal maturation, which implicates more geochemical
71 changes.

72 As coalification proceeds, the carbon content increases, accompanied by a relative depletion in volatile
73 compounds, such as hydrogen and oxygen, emitted in the form of water, methane, carbon dioxide and higher
74 hydrocarbons through decarboxylation and dehydration reactions (Stach and Murchison, 1982). At higher
75 degrees of coalification and temperature, the liquid hydrocarbons formed in previous stages are thermally
76 cracked to methane, increasing the amount of methane produced (Faiz and Hendry, 2006). Peat and brown coal
77 represent the first stage of the coalification process. The vertical pressure exerted by accumulating sediments



78 converts peat into lignite. The intensification of the pressure and heat results in the transition from lignite to
79 bituminous coal, and eventually to anthracite, the highest rank of coal (O'Keefe et al., 2013).

80 During peat and brown coal stages, primary biogenic methane is formed and it is mainly dissolved in water or
81 released during burial, as coal is not appropriately structured for gas retention (Kotarba and Rice, 2001). At
82 more mature stages, thermogenic methane is produced by thermal modification of sedimentary organic matter,
83 which occurs at great depths and intensive heat. Following the basin uplift, methane production can be triggered
84 in the shallower sediments by the meteoric water inflow into the coal (secondary biogenic gas) (Rice, 1993;
85 Scott et al., 1994).

86 The isotopic signature of the methane produced during the coalification process is controlled by the methane
87 origin pathway (Whiticar, 1996). Thermogenic methane is isotopically enriched in ^{13}C (> -50 ‰) compared to
88 biogenic methane, as methanogens preferentially use the lightest isotopes due to the lower bond energy (Rice,
89 1993). Intermediate isotopic compositions of methane might reflect a mixing between microbial and
90 thermogenic gases or secondary processes. Indeed, many controlling factors co-drive the fractionation process,
91 and several contentions about their leverage still persist in literature. Deines (1980) asserts that no significant
92 trend is observed in the isotopic signature of methane in relation to the degree of coalification. Conversely,
93 Chung et al. (1979) observed that the composition of the parent material does affect the isotopic composition of
94 the methane accumulated. While the link between isotopic composition and coal rank is not that straightforward,
95 studies carried out in different worldwide coal seams confirm a stronger relationship between coal bed gas
96 composition and depth. Rice (1993), using data from Australian, Chinese and German coal beds, shows that
97 shallow coal beds tend to contain relatively isotopically lighter methane when compared to those at greater
98 depths. In the presence of intrusions of meteoric water, secondary biogenic methane, isotopically lighter, can be
99 generated and mixed with the thermogenic gas previously produced. Colombo et al. (1966) documented a
100 distinct depth correlation in the Ruhr Basin coal in Germany, with methane becoming more ^{13}C -depleted
101 towards the surface zone, independently from coalification patterns. This tendency can be explained either by
102 bacterial methanogenesis, or by secondary processes such as absorption-desorption of methane. Also Scott
103 (2002), in a study about coal seams in the Bowen Basin, Australia, ascribes the progressive methane ^{13}C -
104 enrichment with depth to the meteoritic recharge in the shallowest seams, associated with a higher bacterial
105 activity and a preferential stripping of ^{13}C - CH_4 by water flow.

106 The migration of methane from the primary zone as a consequence of local pressure release can affect the
107 isotopic composition, since $^{12}\text{CH}_4$ diffuses and desorbs more readily than $^{13}\text{CH}_4$ (Deines, 1980), but the
108 fractionation effect due to migration is less than 1 ‰ (Fuex, 1980). A much larger variation in the isotopic
109 composition is associated with different methanogenic pathways (30 ‰) and thermal maturation stage (25 ‰)
110 (Clayton, 1998). The measurement of Deuterium, coupled with $\delta^{13}\text{CCH}_4$ values, would help to distinguish the
111 pathways of secondary biogenic methane generation, acetoclastic reactions or CO_2 reduction (Faiz and Hendry,
112 2006), but such distinction is beyond the scope of this study.

113 Overall, the $\delta^{13}\text{C}$ values of methane from coal show an extremely wide range and understanding the processes
114 driving the methane isotopic composition needs to focus on the particular set of geological conditions in each
115 sedimentary basin.



116 Here we analyse the isotopic signatures of methane plumes emitted to atmosphere, from the dominant
117 bituminous and anthracite mines in Europe and Australia, of both deep and open cut type, to test the theories of
118 isotopic change due to coal rank and interaction with meteoric water.

119 **2 Material and Methods**

120 **2.1 Coal basins investigated and type of coal exploited**

121 **2.1.1 English and Welsh coal mines**

122 The major coalfields of England and Wales belong to the same stage in the regional stratigraphy of northwest
123 Europe, the Westphalian Stage, between roughly 313 and 304 Ma (Upper Carboniferous). Mining has ceased in
124 many areas. Of those remaining some are located in South Yorkshire (Hatfield and Maltby collieries) (Fig. 1),
125 where 50% of the coalfield's output came from the Barnsley seam, which includes soft coal overlaying a semi-
126 anthracitic coal and bituminous coal in the bottom portion. Seams >2m in thickness are common in the southern
127 half of the Yorkshire coalfield (IMC Group Consulted Limited, 2002). Upper Carboniferous coal measures
128 typical of Yorkshire extend into the East Midlands coalfields. The exposed coalfields are found in the west of
129 this belt, where the coal measures outcrop (roughly from Nottingham to Bradford and Leeds via Chesterfield,
130 Sheffield and Barnsley).

131 The coal exploited in Daw Mill Colliery is part of the Warwickshire Coalfield, from a seam which varies in
132 thickness from 6.6 to 7.5 m (IMC Group Consulted Limited, 2002).

133 The coal of the South Wales basin exhibits a well-defined regional progression in rank, which varies from
134 highly volatile bituminous coal in the south and east margin to anthracite in the north-west part, and the main
135 coal-bearing units reach 2.75 km in thickness toward the south-west of the coalfield (Alderton et al., 2004). The
136 coal is now preferentially extracted in opencast mines, as the extensive exploitation of the coal has left the
137 accessible resources within highly deformed structures (e.g. thrust overlaps, vertical faults) that cannot be
138 worked by underground mining methods (Frodsham and Gayer, 1999). Emissions from two deep mines, Unity
139 and Aberpergwm, were investigated, where mine shafts reach depths up to approximately 750 m
140 (<http://www.wales-underground.org.uk/pit/geology.shtml>).

141 **2.1.2 Upper Silesian Coal Basin in Poland**

142 The Upper Silesian Coal Basin extends from Poland to the Czech Republic and is one of the largest coal basins
143 in Europe, with an area of ~7400 km (Jureczka and Kotas, 1995). The Silesian Region of Poland is estimated to
144 be responsible for significant methane emissions, in the range of 450-1350 Gg annually (Patyńska, 2013). The
145 upper Carboniferous coal-bearing strata of this region are associated with gas deposits of both thermogenic and
146 microbial origin, and the methane content and spatial distribution are coal rank related (Kędzior, 2009) - i.e. the
147 sorption capacity of coal in the basin is found to increase with coal rank. Most of the methane generated during
148 the bituminous stage in the coalification process has escaped from the coal source following basin uplift during
149 Paleogene (Kotarba and Rice, 2001) and diffused through fractures and faults occurring in tectonic zones. The
150 late-stage gas generated by microbial reduction of CO₂ in the coal seams at the top of the Carboniferous
151 sequence accumulated under clay deposition in the Miocene (Kędzior, 2009).



152 2.1.3 Australia: Hunter Coalfield (Sydney Basin)

153 The Hunter Coalfield is part of the Sydney Basin, on the east coast of New South Wales in Australia, and
154 consists of 3 major coal measures. The deepest is the early Permian Greta Coal Measures, which is overlain by
155 the late Permian Whittingham Coal Measures and upper Newcastle Coal Measures. Throughout the Hunter
156 coalfield all sedimentary strata are gently folded, and the same coal seam can be mined at the ground surface
157 and at depths of several hundred meters. In the region surveyed both the opencast and underground mines are
158 extracting coal from the Whittingham coal measures, which are generally high volatile bituminous coals,
159 although some medium to low bituminous coals are extracted (Ward and Kelly, 2013). The mining operation is
160 on a much larger scale than in the UK - the total coal production for the Hunter Coalfield was 123.63 Mt in
161 2011, of which 88.24 Mt was saleable (State of New South Wales, 2013). Several studies have attested to the
162 dispersion of thermogenic methane formed at higher degrees of coalification (i.e. high temperatures and
163 pressures) during the uplift and the subsequent erosion of the basin, followed by the replenishment of the
164 unsaturated basin with more recently formed methane of biogenic (Faiz and Hendry, 2006; Burra, 2010). Gas
165 emplacement is related to sorption capacity of coal strata, in particular to the pore pressure regime, which is
166 influenced by the local geological features (compressional or extensional) of the basin. The south of the Hunter
167 Coalfield is characterized by higher gas content and enhanced permeability than the northern area, with a large
168 potential for methane production, mainly biogenic (Pinetown, 2014).

169 2.2 Sampling and measurement methodology

170 For isotopic characterisation of the methane sources, integrated methane emissions were assessed through
171 detection of the offsite downwind plume. In fact, even when emissions are focused on defined locations, such as
172 vent pipes in underground mines, the methane provenance cannot be localised, since most of collieries are not
173 accessible. For sample collection and measurements of methane emissions downwind of coal mines in the UK
174 and Australia the mobile system described by Zazzeri et al. (2015) has been implemented. The system utilises a
175 Picarro G2301 CRDS (Cavity Ring-Down Spectroscopy) within the survey vehicle, for continuous CH₄ and
176 CO₂ mole fraction measurements, and a mobile module including air inlet, sonic anemometer and GPS receiver
177 on the roof of the vehicle. The entire system is controlled by a laptop, which allows methane mole fractions and
178 the methane plume outline to be displayed in real time on a Google Earth platform during the survey to direct
179 plume sampling. When the plume was encountered, the vehicle was stopped and air samples collected in 3L
180 Tedlar bags, using a diaphragm pump connected to the air inlet. Samples were taken at different locations along
181 the plume transect in order to obtain a wide range of methane mole fractions and isotopic signatures in the
182 collected air. The Upper Silesian basin was surveyed with a Picarro 2101-i measuring continuous CO₂ and CH₄
183 mole fractions and $\delta^{13}\text{C}\text{CO}_2$ isotopic ratio with a precision of 0.3 ‰ in 5 minutes. Samples were collected on site
184 for analysis of $\delta^{13}\text{C}\text{CH}_4$ isotopic ratio.

185 The carbon isotopic ratio ($\delta^{13}\text{C}$) of bag samples was measured in the greenhouse gas laboratory at RHUL (Royal
186 Holloway University of London) in triplicate to high precision (± 0.05 ‰) by continuous flow gas
187 chromatography isotope ratio mass spectrometry (CF GC-IRMS) (Fisher et al., 2006). CH₄ and CO₂ mole
188 fractions of samples were measured independently in the laboratory with a Picarro G1301 CRDS analyser,
189 calibrated against the NOAA (National Oceanic and Atmospheric Administration) WMO-2004A and WMO-
190 X2007 reference scales respectively. The $\delta^{13}\text{C}\text{CH}_4$ signature for each emission plume was calculated using the



191 Keeling plot approach, according to which the $\delta^{13}\text{C}$ isotopic composition of samples and the inverse of the
192 relative mole fractions have a linear relationship, whose intercept represents the isotopic signature of the source
193 (Pataki et al., 2003). Source signatures were provided with the relative uncertainty, computed by the BCES
194 (Bivariate Correlated Errors and intrinsic Scatter) estimator (Akritas and Bershad, 1996), which accounts for
195 correlated errors between two variables and calculates the error on the slope and intercept of the best
196 interpolation line. Mole fraction data and co-located coordinates were used to map the mole fraction variability
197 using the ArcGIS software.

198 3 Results and Discussion

199 While most of the emissions from deep mines come specifically from ventilation shafts, which are point
200 sources, emissions from open-cut mines are wide-spread, and difficult to estimate. However, the objective of
201 this study is not the quantification of emissions, but the assessment of the overall signature of methane released
202 into the atmosphere, made through the sampling of integrated emissions from the whole area. Therefore, even
203 though onsite access to collieries was not possible, by driving around the contiguous area, methane emissions
204 could be intercepted and their mole fractions measured. Table 1 summarises $\delta^{13}\text{CCH}_4$ signatures of all the coal
205 mines and coal basins surveyed with the Picarro mobile system. The English and Welsh coal mines surveyed are
206 shown in Fig. 1.

207 3.1 English coal mines

208 Emissions from Hatfield colliery, one of the few UK deep mines still open at the time of this study, were
209 investigated on 10th July and 26th September 2013. The main seams that have been worked since 1920's are the
210 Barnsley, the Dunsil and the High Hazel seams, at approximate depths of 401-365 m 414-376 and 313-284 m
211 respectively (Hill, 2001). Mole fractions over 7 ppm were recorded during both surveys while transecting the
212 plume (Fig. 2). The methane desorbed from coal heaps within the colliery area and methane vented from shafts
213 might explain the relatively high mole fractions measured. Keeling plots based on the samples collected (4 on
214 the first and 5 on the second survey) give intercept values of -48.3 ± 0.2 and -48.8 ± 0.3 ‰ (2SD).

215 Maltby colliery is one of the largest and deepest mines in England, reaching 991 m in depth, and was closed in
216 March 2013. High volatile bituminous coal was extracted from the Barnsley and Parkgate seams (McEvoy et al.,
217 2006). The coal mine methane was extracted and used for electricity, but over 3 ppm mole fractions were
218 detected in ambient air during both surveys in July and September 2013, giving evidence of methane releases
219 from the recovery system and ventilation shafts. The Keeling plot intercept based on the samples collected in
220 July and in September are -45.9 ± 0.3 and -45.4 ± 0.2 ‰ (2SD) respectively, ~ 3 ‰ heavier for Hatfield Colliery
221 on the same sampling days. Both source signatures are in good agreement with the value of -44.1 ‰ observed
222 for desorbed methane of the Barnsley coal seam, in a study conducted by Hitchman et al. (1990b).

223 Kellingley colliery is a still open deep mine situated in North Yorkshire, which has exploited the Beeston and
224 Silkstone coal seams, characterised by a high quality, low sulphur coal used for coke manufacture. A surface
225 drainage plant for electrical power generation has been implemented (Holloway et al., 2005), and methane
226 releases from the power plant might justify the mole fractions peak of 9 ppm that was observed while driving on



227 the north side of the coal mine on 10th July 2013. The Keeling plot analysis of the samples collected indicates a
228 source signature of -46.5 ± 0.3 ‰ (2SD).

229 Thoresby mine is located in Nottinghamshire and is currently exploiting the Parkgate seam at about 650 m
230 underground. The highest mole fractions detected approached 5 ppm, and 9 samples were collected, giving a
231 source signature of -51.2 ± 0.3 ‰ (2SD).

232 The Daw Mill colliery, before its closure in March 2013, was Britain's biggest coal mine, working the
233 Warwickshire Thick seam, which lies between 500 and 1000 m in depth. The estimated methane content of this
234 seam is low (typically about 1.7 m³/tonne) and, furthermore, a ventilation system is implemented, so that the
235 coal mine methane potential is curtailed (Drake, 1983). During the sampling, the highest methane mole fractions
236 (≈ 5 ppm) were recorded close to the edge of the colliery, whereas, driving downwind of the site at further
237 distances, only background values were measured. Keeling plot analysis reveals a source signature of -51.4 ± 0.2
238 ‰ (2SD).

239 3.2 Welsh coal mines

240 Methane emissions from coal mines in Wales were sampled in order to characterise methane releases from a
241 different rank of coal. The area investigated extended from Cwmllynfell to Merthyr Tydfil (Fig. 1). The South
242 Wales coalfield is estimated to have the highest measured seam gas content in the UK (Creedy, 1991).

243 3.2.1 Deep Mines

244 The deep mine Aberpergwm, which closed in December 2012, did not operate coal mine methane schemes and
245 methane was vented up to the surface as part of standard operation systems (Holloway et al., 2005). That is
246 consistent with methane mole fractions peaks of 6 ppm observed when approaching the colliery. Air samples
247 were also collected near Unity deep mine, Wales' largest drift mine, which reopened in 2007 and is located in
248 the town of Cwmgwrach, only one mile away from Aberpergwm. Isotopic source signatures of 33.3 ± 1.8 ‰ and
249 -30.9 ± 1.4 ‰ result from the Keeling plots based on samples collected respectively near Aberpergwm and Unity
250 colliery, both highly ¹³C enriched relative to all English collieries.

251 3.2.2 Opencast Mines

252 The Picarro mobile system was driven around opencast mines at Cwmllynfell and Abercrave, in the Swansea
253 Valley. Up to 3 ppm methane mole fractions were recorded near the two mines, which were closed in the 1960s
254 as drift mines and are currently exploited as opencast mines. Our measurements confirm that they are still
255 emitting methane, albeit at levels which are not significantly above background. ¹³C signatures between -41.4
256 ± 0.5 and -41.2 ± 0.9 ‰ (2SD) result from isotopic analysis of samples collected downwind of the opencast
257 mines, approximately 10 ‰ lower than the isotopic signature characterizing Welsh deep anthracite mines.

258 3.3 Polish coal mine

259 A Picarro mobile survey of the Upper Silesian basin took place on 10th June 2013 and 12 air samples were
260 collected for isotopic analysis. All the mines in this area are deep mines, exploiting the coal at depths ranging
261 from 300 to 900 m. The Keeling plot analysis includes 8 samples collected around the area of Radoszow,
262 downwind of the KWK Wujek deep mine shafts (white stars in Fig. 4). Methane mole fractions in the range of



263 3-5 ppm were measured in the majority of the area of Katowice and over 20 ppm mole fractions were detected
264 when transecting the plume originating from the exhaust shafts, which confirms the high level of methane that
265 the mine contains. A source signature of -50.9 ± 0.6 ‰ (2SD) was calculated by Keeling plot analysis, which is
266 consistent with the values obtained for the deep mined English bituminous coal.

267 3.4 Australia: Hunter Coalfield

268 On 12th and 18th March 2014 12 samples in total were collected along the route in the Hunter Coalfield, where
269 the bituminous coal strata of the Sydney Basin are extracted both in opencast and underground mines. The
270 methane plume width was in the range of 70 km (Fig. 5a). A maximum mole fraction of 13.5 ppm was measured
271 near a vent shaft associated with the Ravensworth underground mine (see white star in Fig. 5b), which exploits
272 the Lemington, Pikes Gully, Lidell (Upper and Middle) and Barret Seams, the deepest of which is the Barret
273 seam, with a maximum overburden depth of ~350 m (GSS Environmental, 2012). The source signature
274 calculated by the Keeling plot analysis based on all the samples collected during both surveys (grey markers in
275 Fig. 5c) is -66.4 ± 1.3 ‰ (2SD) and this signature likely includes a mixture of methane derived both from
276 underground and opencast mines. Two samples collected downwind of the Ravensworth ventilation shaft (red
277 pushpins in Fig. 5b) fall off the Keeling plot trend for March 2014 and are not included in the calculation,
278 because they are likely dominated by methane from the vent shaft and are not representative of the regional
279 mixed isotopic signature.

280 In January 2016, 10 samples were collected downwind of a ventilation fan in the Bulga mine (second white star
281 in Fig. 5b), aerating underground workings in the Blakefield South Seam, ranging from 130 to 510 m in depth
282 (Bulga Underground Operation mining, 2015). The Keeling plot for these (black circles in Fig. 5c) indicates a
283 $\delta^{13}\text{C}$ source signature of -60.8 ± 0.3 ‰ (2SD). The samples collected next to the Ravensworth ventilation shaft in
284 2014 fit on this Keeling plot, suggesting that the $\delta^{13}\text{CCH}_4$ isotopic signature of emissions from underground
285 works in the Hunter Coalfield is consistent.

286 3.5 New representative $\delta^{13}\text{CCH}_4$ isotopic signatures for coal-derived methane

287 The $\delta^{13}\text{CCH}_4$ isotopic values for coal have been found to be characteristic of single basins, but general
288 assumptions can be made to characterise coal mines worldwide. Table 2 provides the literature $\delta^{13}\text{CCH}_4$ isotopic
289 values characteristic of specific coal basins. The isotopic signatures of emissions from English bituminous coal
290 are consistent with the range of -49 to -31 ‰ suggested by Colombo et al. (1970) for in situ coal bed methane in
291 the Ruhr basin in Germany, which contains the most important German bituminous coal of Upper Carboniferous
292 age and low volatile anthracite (Thomas, 2002). Progression in coal rank might explain the value of -50 ‰ for
293 emissions from English underground mined bituminous coal and -30 ‰ for anthracite deep mines, followed by a
294 5-10 ‰ ^{13}C -depletion caused by the incursion of meteoric water in the basin and the subsequent production of
295 secondary biogenic methane, resulting in -40 ‰ for methane plumes from Welsh open-cut anthracite mines.

296 The link between coal rank and $\delta^{13}\text{CCH}_4$ isotopic signature is appreciable in the study of UK coal mines, but
297 differences in the $^{13}\text{C}/^{12}\text{C}$ isotopic ratio within the same coal sequences can be ascribed to other parameters, such
298 as the depth at which the coal is mined and the occurrence of water incursion. In particular, emissions from
299 Thoresby are more ^{13}C depleted than those measured around Maltby, although both mines exploit the Parkgate
300 seam, meaning that different isotopic signatures cannot be entirely linked to the coal rank. Biogenic methane



301 produced in a later stage due to water intrusion might have been mixed with the original thermogenic methane
302 formed during the coalification process.

303 Differences in methane emissions and their isotopic signature between opencast and deep mines have been
304 assessed by surveying both surface and underground mines, in the Welsh anthracite belt, and in the Hunter
305 Coalfield. The shallower deposits have been more exposed to the weathering and meteoric water, most likely
306 associated with the production of some isotopically lighter microbial methane. Mole fractions up to 2.5 ppm
307 were measured around opencast mines in the Hunter Coalfield, in Australia, within a methane plume of more
308 than 70 km width. The highest methane mole fractions were consistently measured downwind of vent shafts in
309 underground mines. The difference in the source isotopic signature for methane emissions between the two
310 types of mining in the Hunter Coalfield (from -61 to -66 ‰) and in Wales (from -31 to -41 ‰) reflects the
311 isotopic shift of 5-10 ‰ that has been attributed to the occurrence of secondary biogenic methane.

312 The $\delta^{13}\text{C}$ signatures for coalbed methane emissions from the Upper Silesian basin are highly variable, with the
313 most ^{13}C depleted methane associated with diffusion processes or secondary microbial methane generation
314 (Kotarba and Rice, 2001), but the value of -51 ‰ measured for methane emissions from the KWK Wujek deep
315 mine is consistent with the value of -50 ‰ inferred for emissions from English bituminous coal extracted in
316 underground mines.

317 4 Conclusions

318 By measuring the isotopic signatures of methane plumes from a representative spread of coal types and depths,
319 we show that the $\delta^{13}\text{C}$ isotopic value to be included in regional and global atmospheric models for the estimate
320 of methane emissions from the coal sector must be chosen according to coal rank and type of mining (opencast
321 or underground). For low resolution methane modelling studies an averaged value of -65 ‰ is suggested for
322 bituminous coal exploited in open cast mines and of -55 ‰ in deep mines, whereas values of -40 ‰ and -30 ‰
323 can be assigned to anthracite opencast and deep mines respectively.

324 Global methane budget models that incorporate isotopes have used a $\delta^{13}\text{C}$ signature of -35 ‰ for coal or a value
325 -40 ‰ for total fossil fuels (e.g. Hein et al., 1997; Mikaloff Fletcher et al., 2004; Bousquet et al., 2006; Monteil
326 et al., 2011), but, given the relative rarity of anthracite coal reserves and the dominance of bituminous coal
327 (<http://www.transparencymarketresrch.com/anthracite-coal-mining.html>), it seems likely that a global average
328 emission from coal mining activities will be lighter, with the -50 ‰ recorded for deep-mined bituminous coal in
329 Europe being a closer estimate. However, for detailed global modelling of atmospheric methane, isotopic
330 signatures of coal emissions should be region or nation specific, as greater detail is needed given the wide global
331 variation. The assignment of an incorrect global mean, or a correct global mean but inappropriate for regional
332 scale modelling, might lead to incorrect emissions estimates or source apportionment. The new scheme gives the
333 possibility for an educated estimate of the $\delta^{13}\text{C}$ signature of emission to atmosphere to be made for an individual
334 coal basin or nation, given information on the type of coal being mined and the method of extraction.

335 In conclusion, high-precision measurements of $\delta^{13}\text{C}$ in plumes of methane emitted to atmosphere from a range
336 of coal mining activities have been used to constrain the isotopic range for specific ranks of coal and mine type,
337 offering more representative isotopic signatures for use in methane budget assessment at regional and global
338 scales.



339 **Acknowledgements**

340 Giulia Zazzeri would like to thank Royal Holloway, University of London for provision of a Crossland
341 scholarship and a contribution from the Department of Earth Sciences from 2011 to 2014. Analysis of samples
342 from Poland was funded through the European Community's Seventh Framework Programme (FP7/2007-2013)
343 in the InGOS project under grant agreement n. 284274. Sampling in Australia was possible due to a grant from
344 the Cotton Research and Development Corporation.

345 **References**

- 346 Akritas, M.G., and Bershad, M.A., 1996, Linear regression for astronomical data with measurement errors and
347 intrinsic scatter: *Astrophysical Journal*, v. 470, p. 706-714.
- 348 Alderton, D., Oxtoby, N., Brice, H., Grassineau, N., and Bevens, R., 2004, The link between fluids and rank
349 variation in the South Wales Coalfield: evidence from fluid inclusions and stable isotopes: *Geofluids*, v. 4,
350 p. 221-236.
- 351 Aravena, R., Harrison, S., Barker, J., Abercrombie, H., and Rudolph, D., 2003, Origin of methane in the Elk
352 Valley coalfield, southeastern British Columbia, Canada: *Chemical Geology*, v. 195, p. 219-227.
- 353 Bousquet, P., Ciais, P., Miller, J., Dlugokencky, E., Hauglustaine, D., Prigent, C., Van der Werf, G., Peylin, P.,
354 Brunke, E.-G., and Carouge, C., 2006, Contribution of anthropogenic and natural sources to atmospheric
355 methane variability: *Nature*, v. 443, p. 439-443.
- 356 Bulga Underground Operations Mining: Operation Plan 2015 to 2021, 2015.
- 357 Burra, A., 2010, Application of domains in gas-in-place estimation for opencut coal mine fugitive gas emissions
358 reporting, Bowen Basin Symposium, p. 59-64.
- 359 Chung, H.M., and Sackett, W.M., 1979, Use of stable carbon isotope compositions of pyrolytically derived
360 methane as maturity indices for carbonaceous materials: *Geochimica et Cosmochimica Acta*, v. 43, no.12.
- 361 Clayton, J., 1998, Geochemistry of coalbed gas—A review: *International Journal of Coal Geology*, v. 35, p. 159-
362 173.
- 363 Colombo U., G.F., Gonfiantini F., Gonfiantini R., Kneuper G., Teichmuller I., Teichmuller R. , 1970, Carbon
364 isotope study on methane from German coal deposits.: *Advances in Organic Geochemistry 1966* (eds G. D.
365 HOBSON and G. C. SPEERS), p. 1-26.
- 366 Creedy, D.P., 1991, An introduction to geological aspects of methane occurrence and control in British deep
367 coal mines: *Quarterly Journal of Engineering Geology*, v. 24, p. 209-220.
- 368 Dai, J.X., Qi, H.F., Song, Y., and Guan, D.S., 1987, Composition, carbon isotope characteristics and the origin
369 of coal-bed gases in China and their implication: *Scientia Sinica Series B-Chemical Biological
370 Agricultural Medical & Earth Sciences*, v. 30, p. 1324-1337.
- 371 Deines, P., 1980, The isotopic composition of reduced organic carbon: *Handbook of environmental isotope
372 geochemistry*, p. 329-406.
- 373 Drake, D., 1983, *Working the Warwickshire Thick Coal, Improved Techniques for the Extraction of Primary
374 Forms of Energy*, Springer Netherlands, p. 156-156.
- 375 Faiz, M., and Hendry, P., 2006, Significance of microbial activity in Australian coal bed methane reservoirs—a
376 review: *Bulletin of Canadian Petroleum Geology*, v. 54, p. 261-272.



- 377 Fisher, R., Lowry, D., Wilkin, O., Sriskantharajah, S., and Nisbet, E.G., 2006, High-precision, automated stable
378 isotope analysis of atmospheric methane and carbon dioxide using continuous-flow isotope-ratio mass
379 spectrometry: *Rapid Communications in Mass Spectrometry*, v. 20, p. 200-208.
- 380 Flores, R.M., Rice, C.A., Stricker, G.D., Warden, A., and Ellis, M.S., 2008, Methanogenic pathways of coal-bed
381 gas in the Powder River Basin, United States: the geologic factor: *International Journal of Coal Geology*,
382 v. 76, p. 52-75.
- 383 Frodsham, K., and Gayer, R., 1999, The impact of tectonic deformation upon coal seams in the South Wales
384 coalfield, UK: *International Journal of Coal Geology*, v. 38, p. 297-332.
- 385 Fuex, A., 1980, Experimental evidence against an appreciable isotopic fractionation of methane during
386 migration: *Physics and Chemistry of the Earth*, v. 12, p. 725-732.
- 387 Fung, I., John, J., Lerner, J., Matthews, E., Prather, M., Steele, L., and Fraser, P., 1991, Three-dimensional
388 model synthesis of the global methane cycle: *Journal of Geophysical Research*, v. 96, no.D7.
- 389 GSS Environmental, 2012, Ravensworth Underground Mine: Liddell Seam Project.
- 390 Hein, R., Crutzen, P.J., and Heimann, M., 1997, An inverse modeling approach to investigate the global
391 atmospheric methane cycle: *Global Biogeochemical Cycles*, v. 11, p. 43-76.
- 392 Hill, A., 2001, *The South Yorkshire Coalfield: A History and Development*, Tempus Books, Gloucestershire.
- 393 Hitchman, S., Darling, W., and Williams, G., 1990a, Stable isotope ratios in methane containing gases in the
394 United Kingdom.
- 395 Hitchman, S., Darling, W., and Williams, G., 1990b, Stable isotope ratios in methane containing gases in the
396 United Kingdom. Report of the British Geological Survey, Processes Research Group WE/89/30.
- 397 Holloway, S., Jones, N., Creedy, D., and Garner, K., 2005, Can new technologies be used to exploit the coal
398 resources in the Yorkshire-Nottinghamshire coalfield?: *Carboniferous Hydrocarbon Geology: The*
399 *Southern North Sea Surrounding Areas*, v. 7 Occasional publications of the Yorkshire Geological Society,
400 p. 195–208.
- 401 IMC Group Consulting Limited, 2002, A review of the remaining reserves at deep mines for the Department of
402 Trade and Industry.
- 403 IPCC, 2006, 2006 IPCC guidelines for national greenhouse gas inventories: industrial processes and product
404 use, Kanagawa, JP: Institute for Global Environmental Strategies.
- 405 Jureczka, J., and Kotas, A., 1995, Coal deposits—Upper Silesian Coal Basin: The carboniferous system in
406 Poland, v. 148, p. 164-173.
- 407 Kanduč, T., Grassa, F., Lazar, J., and Zavšek, S., 2015, Geochemical and isotopic characterization of coalbed
408 gases in active excavation fields at Preloge and Pesje (Velenje Basin) mining areas: *RMZ–M&G*, v. 62, p.
409 21-36.
- 410 Kędzior, S., 2009, Accumulation of coal-bed methane in the south-west part of the Upper Silesian Coal Basin
411 (southern Poland): *International Journal of Coal Geology*, v. 80, p. 20-34.
- 412 Kotarba, M.J., and Rice, D.D., 2001, Composition and origin of coalbed gases in the Lower Silesian basin,
413 southwest Poland: *Applied Geochemistry*, v. 16, p. 895-910.
- 414 Levin, I., Bergamaschi, P., Dörr, H., and Trapp, D., 1993, Stable isotopic signature of methane from major
415 sources in Germany: *Chemosphere*, v. 26, p. 161-177.



- 416 Liptay, K., Chanton, J., Czepiel, P., and Mosher, B., 1998, Use of stable isotopes to determine methane
417 oxidation in landfill cover soils: *Journal of Geophysical Research: Atmospheres* (1984–2012), v. 103, p.
418 8243-8250.
- 419 Locatelli, R., Bousquet, P., Chevallier, F., Fortems-Cheney, A., Szopa, S., Saunois, M., Agusti-Panareda, A.,
420 Bergmann, D., Bian, H., and Cameron-Smith, P., 2013, Impact of transport model errors on the global and
421 regional methane emissions estimated by inverse modelling: *Atmospheric chemistry and physics*, v. 13, p.
422 9917-9937.
- 423 Lowry, D., Holmes, C.W., Rata, N.D., O'Brien, P., and Nisbet, E.G., 2001, London methane emissions: Use of
424 diurnal changes in concentration and $\delta^{13}\text{C}$ to identify urban sources and verify inventories: *Journal of*
425 *Geophysical Research: Atmospheres*, v. 106, p. 7427-7448.
- 426 McEvoy F. M., M.D., Harrison D.J., Cameron D.G., Burke H.F., Spencer N.A., Evans D.J., Lott G.K., Hobbs
427 S.F. and Highley D.E., 2006, Mineral Resource Information in Support of National, Regional and Local
428 Planning: South Yorkshire (comprising Metropolitan Boroughs of Barnsley, Doncaster and Rotherham
429 and City of Sheffield) British Geological Survey Commissioned Report.
- 430 Mikaloff Fletcher, S.E., Tans, P.P., Bruhwiler, L.M., Miller, J.B., and Heimann, M., 2004, CH_4 sources
431 estimated from atmospheric observations of CH_4 and its $^{13}\text{C}/^{12}\text{C}$ isotopic ratios: 2. Inverse modeling of
432 CH_4 fluxes from geographical regions: *Global Biogeochemical Cycles*, v. 18, no.4.
- 433 Miller, J.B., 2004, The carbon isotopic composition of atmospheric methane and its constraints on the global
434 methane budget, *Stable Isotopes and Biosphere-Atmosphere Interactions: Processes and Biological*
435 *Controls*, Elsevier Academic Press California, p. 288-306.
- 436 Monteil, G., Houweling, S., Dlugokenky, E., Maenhout, G., Vaughn, B., White, J., and Rockmann, T., 2011,
437 Interpreting methane variations in the past two decades using measurements of CH_4 mixing ratio and
438 isotopic composition: *Atmospheric chemistry and physics*, v. 11, p. 9141-9153.
- 439 Nisbet, E.G., Dlugokenky, E.J., and Bousquet, P., 2014, Methane on the rise—again: *Science*, v. 343, p. 493-
440 495.
- 441 O'Keefe, J.M., Bechtel, A., Christanis, K., Dai, S., DiMichele, W.A., Eble, C.F., Esterle, J.S., Mastalerz, M.,
442 Raymond, A.L., and Valentim, B.V., 2013, On the fundamental difference between coal rank and coal
443 type: *International Journal of Coal Geology*, v. 118, p. 58-87.
- 444 Papendick, S.L., Downs, K.R., Vo, K.D., Hamilton, S.K., Dawson, G.K., Golding, S.D., and Gilcrease, P.C.,
445 2011, Biogenic methane potential for Surat Basin, Queensland coal seams: *International Journal of Coal*
446 *Geology*, v. 88, p. 123-134.
- 447 Pataki, D.E., Bowling, D.R., and Ehleringer, J.R., 2003, Seasonal cycle of carbon dioxide and its isotopic
448 composition in an urban atmosphere: Anthropogenic and biogenic effects: *Journal of Geophysical*
449 *Research-Atmospheres*, v. 108, no.D23.
- 450 Patyńska, R., 2013, Prognoza wskaźników emisji metanu z kopalń metanowych węgla kamiennego w Polsce:
451 *Polityka Energetyczna*, v. 16.
- 452 Pinetown, K., 2014, Regional coal seam gas distribution and burial history of the Hunter Coalfield, Sydney
453 Basin: *Australian Journal of Earth Sciences*, v. 61, p. 409-426.
- 454 Qin, S., Tang, X., Song, Y., and Wang, H., 2006, Distribution and fractionation mechanism of stable carbon
455 isotope of coalbed methane: *Science in China Series D: Earth Sciences*, v. 49, p. 1252-1258.



- 456 Rice, D.D., 1993, Composition and origins of coalbed gas: Hydrocarbons from coal: AAPG Studies in Geology,
457 v. 38, p. 159-184.
- 458 Rice, D.D., Clayton, J.L., and Pawlewicz, M.J., 1989, Characterization of coal-derived hydrocarbons and
459 source-rock potential of coal beds, San Juan Basin, New Mexico and Colorado, USA: International Journal
460 of Coal Geology, v. 13, p. 597-626.
- 461 Scott, A.R., 2002, Hydrogeologic factors affecting gas content distribution in coal beds: International Journal of
462 Coal Geology, v. 50, p. 363-387.
- 463 Scott, A.R., Kaiser, W., and Ayers Jr, W.B., 1994, Thermogenic and secondary biogenic gases, San Juan Basin,
464 Colorado and New Mexico--implications for coalbed gas producibility: AAPG bulletin, v. 78, p. 1186-
465 1209.
- 466 Smith, J.W., Gould, K., and Rigby, D., 1981, The stable isotope geochemistry of Australian coals: Organic
467 Geochemistry, v. 3, p. 111-131.
- 468 Stach, E., and Murchison, D.G., 1982, Stach's Textbook of coal petrology, Borntraeger, Stuttgart (1982), 426 p.
469 State of New South Wales, Department of Trade & Investment, Division of Resources & Energy (2013). 2013
470 New South Wales Coal Industry profile.
- 471 Thomas, L., 2002, Coal geology, John Wiley & Sons.
- 472 Townsend-Small, A., Tyler, S.C., Pataki, D.E., Xu, X.M., and Christensen, L.E., 2012, Isotopic measurements
473 of atmospheric methane in Los Angeles, California, USA: Influence of "fugitive" fossil fuel emissions:
474 Journal of Geophysical Research-Atmospheres, v. 117, no.D7.
- 475 U.S. EPA, 2013, US Environmental Protection Agency, Global Mitigation of Non-CO₂ Greenhouse Gases:
476 2010–2030, USEPA, Washington, DC EPA-430-R-13-011.
- 477 Waldron, S., Fallick, A., and Hall, A., 1998, Comment on" Spatial distribution of microbial methane production
478 pathways in temperate zone wetland soils: Stable carbon and hydrogen evidence" by ERC Hornibrook, FJ
479 Longstaffe, and WS Fyfe: Geochimica et Cosmochimica Acta, v. 62, p. 369-372.
- 480 Ward, C., and Kelly, B.F.J., 2013, Background Paper on New South Wales Geology: with a focus on basins
481 containing coal seam gas resources., UNSW Global, The University of New South Wales, a report
482 prepared for the Office of the NSW Chief Scientist and Engineer.
- 483 Whiticar, M., and Schaefer, H., 2007, Constraining past global tropospheric methane budgets with carbon and
484 hydrogen isotope ratios in ice: Philosophical Transactions of the Royal Society of London A:
485 Mathematical, Physical and Engineering Sciences, v. 365, p. 1793-1828.
- 486 Whiticar, M.J., 1996, Stable isotope geochemistry of coals, humic kerogens and related natural gases:
487 International Journal of Coal Geology, v. 32, p. 191-215.
- 488 Whiticar, M.J., 1999, Carbon and hydrogen isotope systematics of bacterial formation and oxidation of methane:
489 Chemical Geology, v. 161, p. 291-314.
- 490 Zazzeri, G., Lowry, D., Fisher, R., France, J., Lanoisellé, M., and Nisbet, E., 2015, Plume mapping and isotopic
491 characterisation of anthropogenic methane sources: Atmospheric Environment, v. 110, p. 151-162.
- 492



493

494

Sampling Site	Country	Sampling Date	$\delta^{13}\text{C}$ Signatures [‰]	Samples number used in Keeling plots
Kellingley Colliery	North Yorkshire/UK	Sept-2013	-46.5 ± 0.3	5
Maltby Colliery	South Yorkshire/UK	Jul-2013	-45.9 ± 0.3	3
		Sept-2013	-45.4 ± 0.2	4
Hatfield Colliery	South Yorkshire/UK	Jul-2013	-48.3 ± 0.2	4
		Sept-2013	-48.8 ± 0.3	5
Thoresby Colliery	Nottinghamshire/UK	Nov-2013	-51.2 ± 0.3	9
Daw Mill Colliery	Warwickshire/UK	Nov-2013	-51.4 ± 0.2	4
Cwmllynfell Colliery	Wales/UK	Oct-2013	-41.2 ± 0.9	4
Abercrave Colliery	Wales/UK	Oct-2013	-41.4 ± 0.5	5
Aberpergwm Colliery	Wales/UK	Oct-2013	-33.3 ± 1.8	3
Unity Colliery	Wales/UK	Oct-2013	-30.9 ± 1.4	5
Hunter Coalfield	Australia	Mar-2014	-66.4 ± 1.3	12
Bulga Colliery	Australia	Jan-2016	-60.8 ± 0.3	10
Boggabri and Tarrawonga Collieries	Australia	Mar-2014	-55.5 ± 1.3	5
Upper Silesian Basin	Poland	Jun-2013	-50.9 ± 1.2	8

495

496

Table 1 $\delta^{13}\text{CCH}_4$ Signatures of all the coal mines and coal basins surveyed with the Picarro mobile system. Errors in the $\delta^{13}\text{C}$ Signatures are calculated as 2 standard deviations.



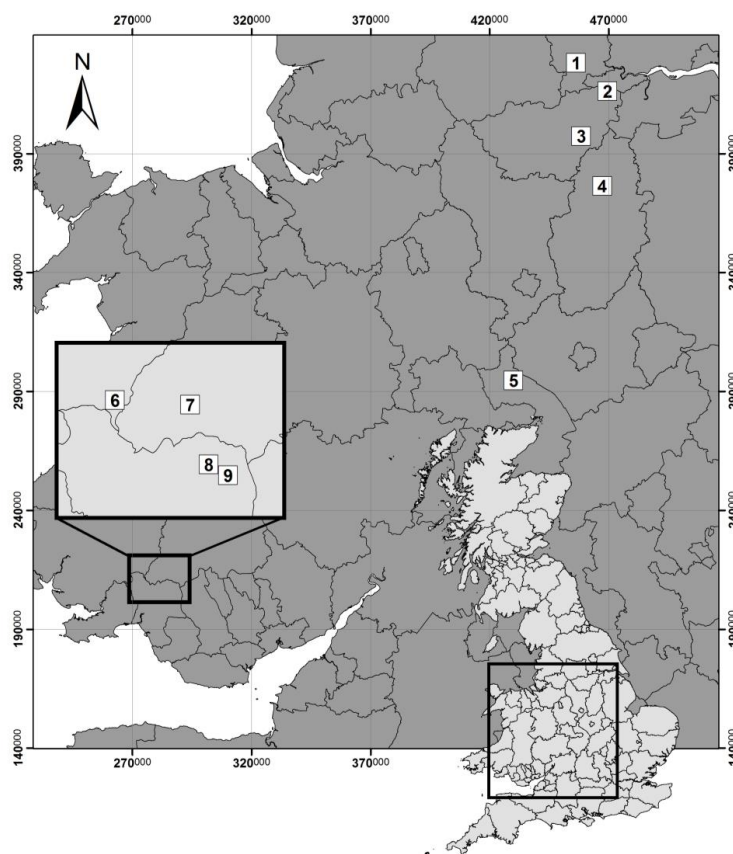
Site	Coal Rank	$\delta^{13}\text{C}$ (‰)	Author	$\delta^{13}\text{C}$ (‰) measured in this study
Velenje Basin, Slovenia	Lignite	-71.8 to -43.4	Kanduč et al. (2015)	
Australia	From brown coal to low volatile bituminous coal.	-73.0 to -43.5	Smith et al. (1981)	-66.4 ± 1.3 to -55.5 ± 1.3
Powder River Basin, U.S.A.	Sub-bituminous coal	-68.4 to -59.5	Flores et al. (2008)	
Queensland Basin, Australia	From Sub-bituminous to high volatile bituminous	-57.3 to -54.2	Papendick et al. (2011)	
San Juan basin, New Mexico and Colorado	High-volatile Bituminous coal	-43.6 to -40.5	Rice et al. (1989)	
Elk Valley Coalfield, British Columbia	Bituminous coal	-65.4 to -51.8	Aravena et al. (2003)	
UK, Barnsley seam	Bituminous coal	-44.1	Hitchman et al. (a, b)	-48.8 ± 0.3 to -45.4 ± 0.2
Upper Silesian Coal Basin, Poland	Sub-bituminous coal to anthracite	-79.9 to -44.5	Kotarba and Rice (2001)	-50.9 ± 0.6
Eastern China	Sub-bituminous to anthracite	-66.9 to -24.9	Dai et al. (1987)	
Ruhr basin, Germany	Bituminous coal, Anthracite	-37 (-60 to -14)	Deines (1980)	
Western Germany	High-volatile bituminous to anthracite.	-70.4 to -16.8	Colombo et al. (1970)	
Qinshui, China	Anthracite	-41.4 to -34.0	Qin et al. (2006)	
Wales, UK	Anthracite			-33.3 ± 1.8 to -30.9 ± 1.4

 497 **Table 2 Literature isotope values obtained by methane samples from boreholes and coal seams. Errors are not included in the sources.**



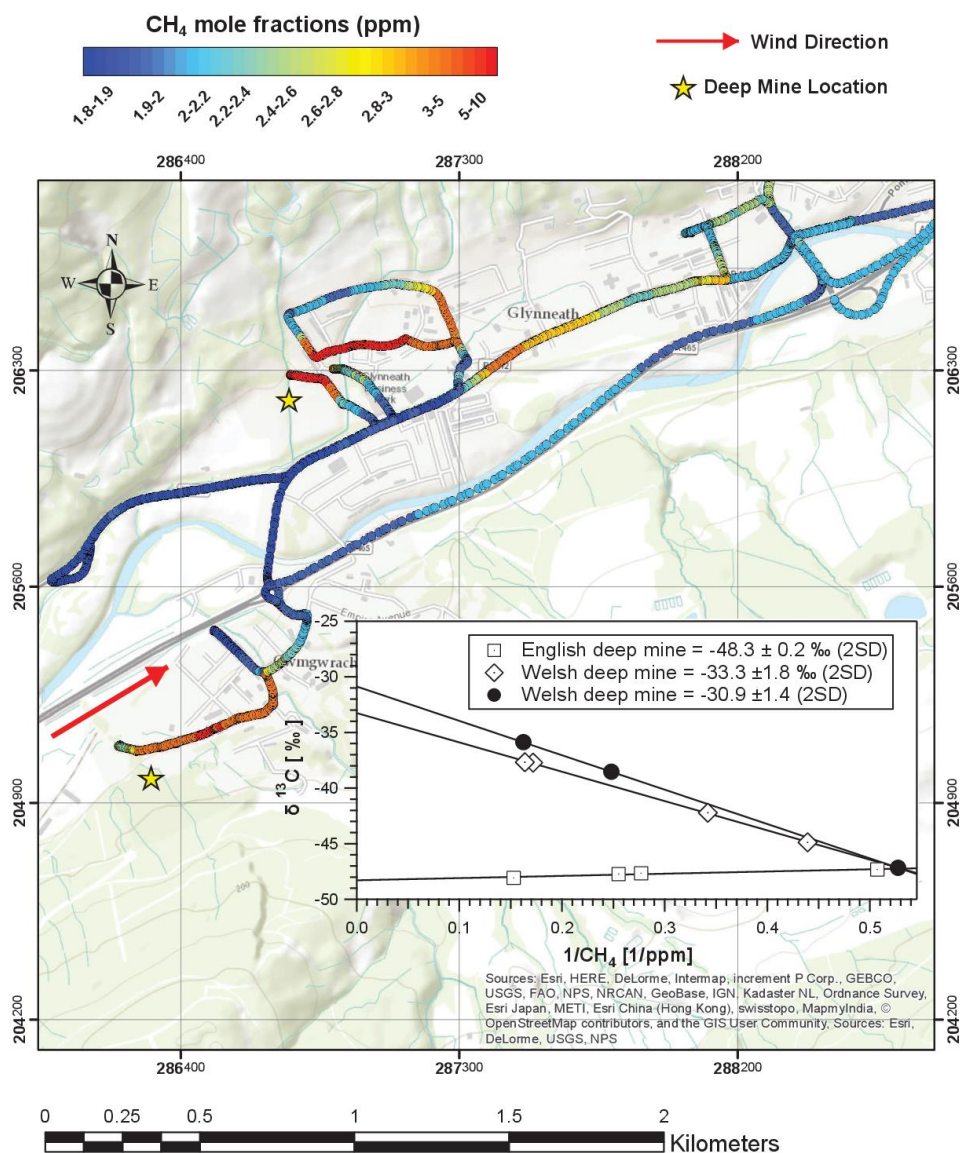
498

499



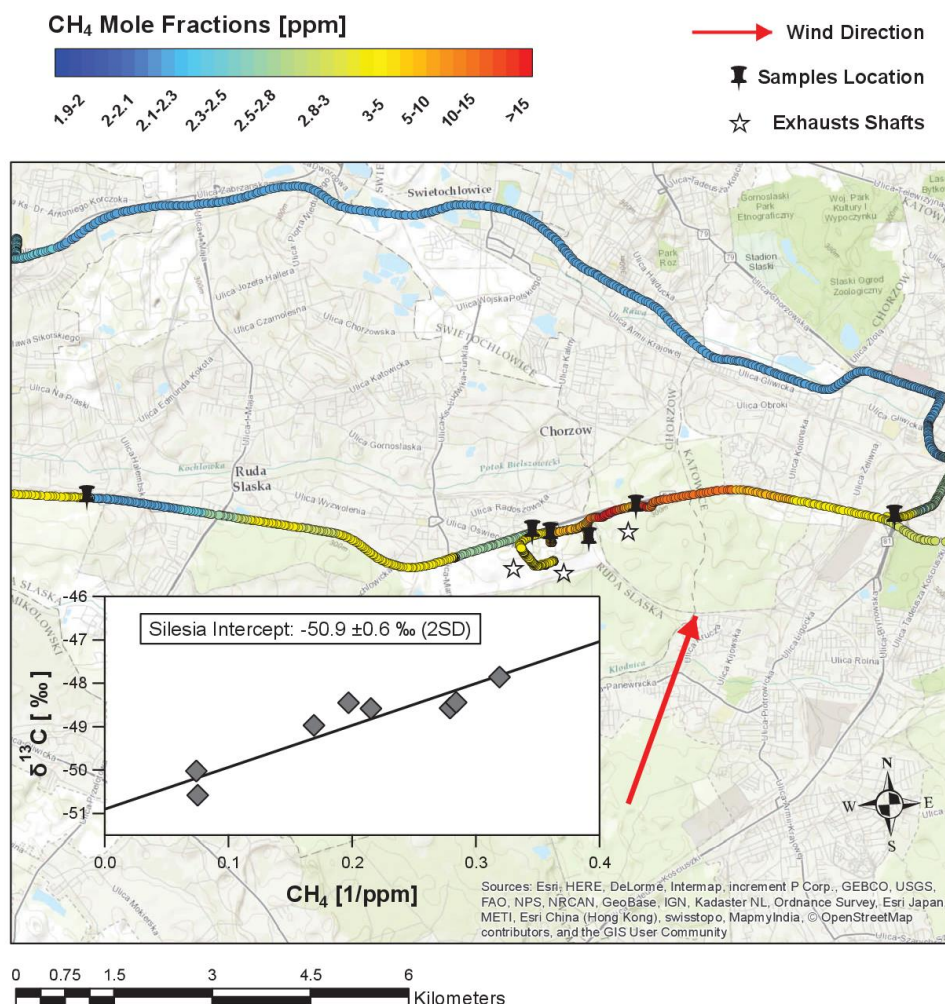
500

501 **Figure 1** Location of English coal mines (1 Kellingley, 2 Hatfield, 3 Maltby, 4 Thoresby, 5 Daw Mill) and Welsh coal
502 mines in the anthracite belt (6 Cwmllynfell, 7 Abercrave, 8 Unity, 9 Aberpergwm). Coordinates are displayed in the
503 National British Coordinates System.



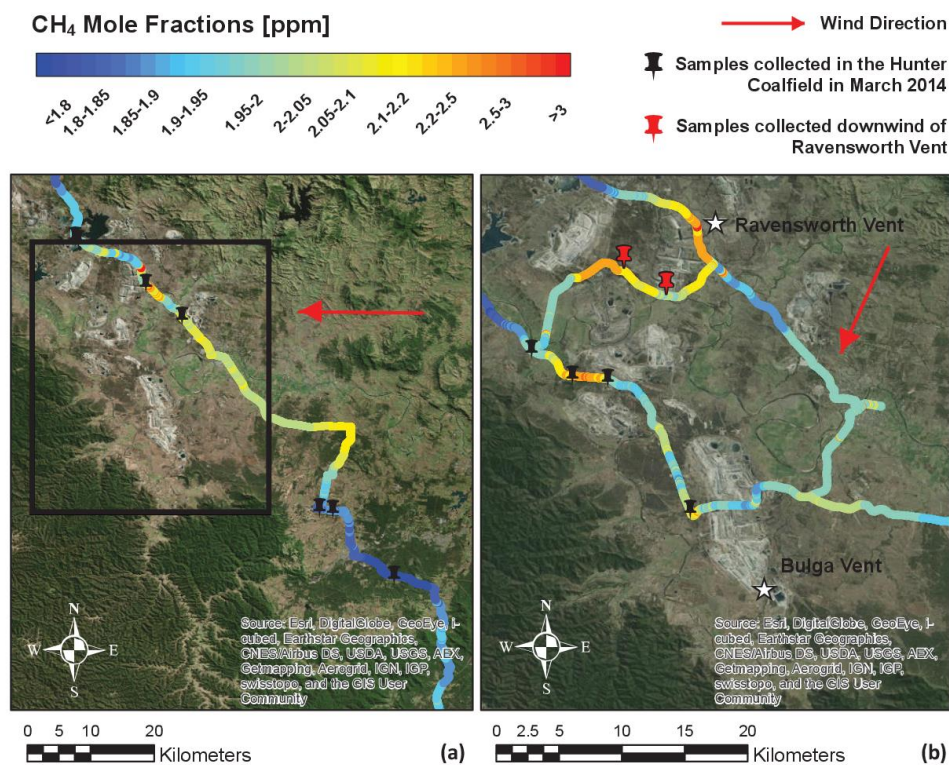
507

508 **Figure 3** ArcGIS plot of methane mole fractions recorded in October 2013 next to Aberpergwm and Unity deep
 509 mines in Wales –yellow stars. Grid Coordinates are displayed in the National British Coordinate System. The
 510 embedded graph is the Keeling plot based on samples collected downwind of one English coal mine (Hatfield
 511 Colliery) and two Welsh deep mines (Aberpergwm and Unity Colliery). Errors on the y-axis are within 0.05 ‰
 512 and on the x-axis 0.0001 ppm⁻¹, and are not noticeable on the graph.



513

514 **Figure 4** ArcGIS map of methane mole fractions recorded in the Upper Silesian basin in June 2013. White stars
 515 represent the KWK Wujek deep mine exhausts shafts. The embedded graph is the Keeling Plot based on samples
 516 collected downwind the KWK Wujek deep mine in June 2013. Errors on the y-axis are within 0.05 ‰ and on the x-axis
 517 0.0001 ppm⁻¹, and are not noticeable on the graph.



518

519 **Figure 5** Methane mole fractions recorded in the Hunter Coalfield on 12th March 2014 (a) and during a more
 520 detailed survey of the area highlighted by the black square on 18th March 2014 (b). Keeling plot based on samples
 521 collected along the route in the Hunter Coalfield in March 2014 (grey and red markers) and near to ventilation in
 522 January 2016 (black markers) (c). Errors on the y-axis are within 0.05 ‰ and on the x-axis 0.0001 ppm⁻¹, and are not
 523 noticeable on the graph.

524

525